



Toward architecturing of metal composites by twist extrusion

Marat I. Latypov, Yan Beygelzimer, Roman Kulagin, Victor Varyukhin & Hyoung Seop Kim

To cite this article: Marat I. Latypov, Yan Beygelzimer, Roman Kulagin, Victor Varyukhin & Hyoung Seop Kim (2015) Toward architecturing of metal composites by twist extrusion, Materials Research Letters, 3:3, 161-168, DOI: [10.1080/21663831.2015.1034812](https://doi.org/10.1080/21663831.2015.1034812)

To link to this article: <http://dx.doi.org/10.1080/21663831.2015.1034812>



© 2015 The Author(s). Published by Taylor & Francis.



Published online: 14 May 2015.



Submit your article to this journal [↗](#)



Article views: 500



View related articles [↗](#)





View Crossmark data [↗](#)



Citing articles: 1 View citing articles [↗](#)

Toward architecturing of metal composites by twist extrusion

Marat I. Latypov^{a,*} , Yan Beygelzimer^{b*}, Roman Kulagin^{b,c}, Victor Varyukhin^b and Hyoung Seop Kim^{a,d*} 

^aCenter for Advanced Aerospace Materials, POSTECH, Pohang, Republic of Korea; ^bDonetsk Institute for Physics and Engineering named after A.A. Galkin, National Academy of Sciences of Ukraine, Kyiv, Ukraine; ^cInstitute of Nanotechnology, Karlsruhe Institute of Technology (KIT), Karlsruhe, Germany; ^dDepartment of Materials Science and Engineering, POSTECH, Pohang 790–784, Republic of Korea

(Received 23 February 2015; final form 24 March 2015)

The paper presents a new route for realizing the concept of architecturing of composites by severe plastic deformation. The proposed route involves multi-pass twist extrusion of a composite with fibers. The potential of the method is first illustrated by mathematical modeling and then tested through pilot processing of a composite consisting of a copper matrix and a single aluminum fiber. Metallographic analysis revealed an unexpected shape of the fiber after processing. Finite element simulations were performed to understand the evolution of the fiber shape and to optimize the processing regime for achieving improved reinforcements in twist-extruded composites.

Keywords: Architected Materials, Severe Plastic Deformation, Twist Extrusion, Metal Composites

Introduction Architecturing of materials is an emerging and promising approach to intelligent material design. It was proposed as a concept of material development that combines the viewpoints of metallurgists, who aim at microstructure optimization, and structural mechanicians, who focus on shape optimization.[1,2] Architected materials thus suppose that the presence of microstructural features, their shape, and spatial arrangement are all consistently tailored for improved overall performance of the material. Producing such materials frequently requires microstructural or compositional gradients and microstructure control at multiple length scales.[1,2]

As a result of considerate design, architected materials reveal improved properties and are able to serve multiple functions. Materials with gradient nanostructures,[3–5] corrugated [6] or interlocking [7] composites, and natural materials [8–10] are just a few examples illustrating how superior properties and multi-functionality can be gained through architecturing. Another virtue of architected materials is that they help filling the holes in the property space (‘Ashby plot’).[11,12]

Recognizing the potential of two concepts, architecturing and severe plastic deformation (SPD), Bouaziz et al. [13] proposed architecturing of materials by SPD. The main motivation for architecturing by SPD methods is to accompany architecturing by nanostructuring as SPD allows for significant microstructure refinement. Since SPD alone is a powerful approach for improvement of material properties,[14–16] the concept of architecturing by SPD promises new horizons of novel and improved combinations of properties of materials.

Despite the potential, the idea of architecturing by SPD has enjoyed little practice so far. Furthermore, the feasibility of the concept was supported mostly by finite element (FE) simulations [13] without practical realization. In this context, SPD routes capable of architecturing are necessary to realize and test the theoretical ideas. With this motivation, we propose a way of utilizing multi-pass twist extrusion (TE) as an SPD route for producing bulk architected materials. Specifically, in this paper, we first present theoretical prerequisites for architecturing by TE and then demonstrate the feasibility of the approach through manufacturing a composite with a copper matrix and a single aluminum fiber. Finally, FE

*Corresponding authors. Emails: yanbeygel@gmail.com, hskim@postech.ac.kr

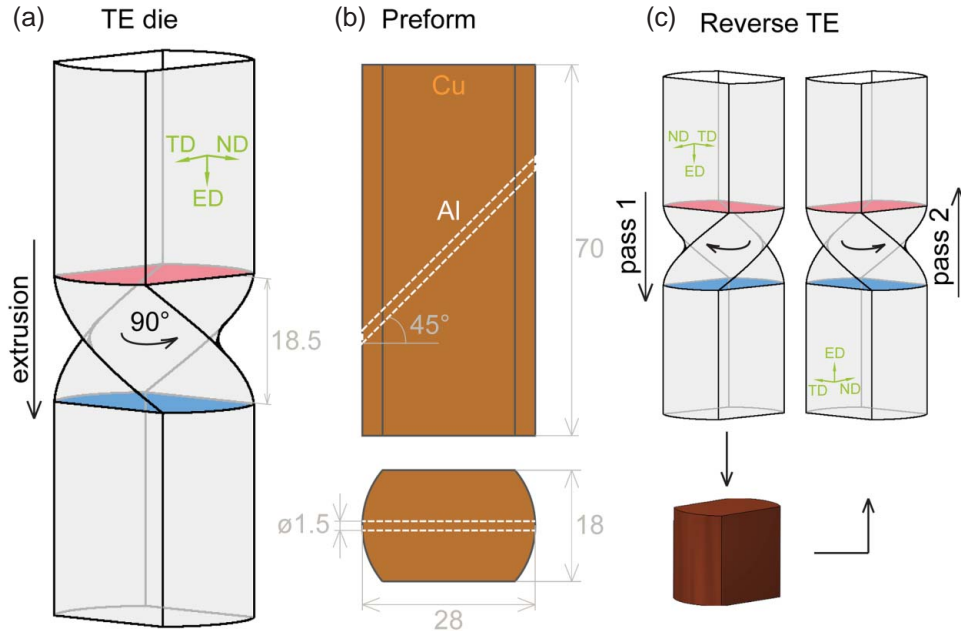


Figure 1. Schematics of (a) TE die and (b) preform composite utilized in the current experiments; (c) illustration of prospective process of reverse TE with alternating sense of twisting proposed based on the FE analysis (Finite element modelling section).

simulations were performed to support the experimental data for a better understanding of the evolution of the fiber shape during multi-pass TE as well as to optimize the process for achieving improved reinforcements.

Background TE is an SPD method introduced with the motivation to process large samples by a deformation regime similar to high-pressure torsion.[17] In TE, a prismatic sample is pressed through a die consisting of three channels: straight entry channel, twist channel, and straight exit channel (Figure 1(a)). The prevailing deformation mode in TE is simple shear in two plastic deformation zones near the transients between the twist and straight channels (highlighted in Figure 1(a)).[18,19] Since the die profile is the same in all channels, the overall shape of the sample after the process can be preserved by the virtue of backward pressure. As a result, multiple passes can be performed on the same sample for accumulating large plastic strains in the material.

Owing to the peculiar shape of the TE die, deformation in TE is complex and non-monotonic. To describe deformation in TE, Beygelzimer et al. [17] proposed an analytical model in which the material flow is decomposed into two terms: ideal deformation (helical flow) and deviations therefrom (cross flow). For simplicity, it is often assumed that the total flow can be approximated to the ideal helical flow, whereas deviations (i.e. cross flow) can be neglected.[17] In this approximation, which was later termed as the simple shear model of TE, deformation in TE is idealistically viewed as a sequence of shearing–reverse shearing at two intersection planes of the TE die.[18]

The simple shear model concisely describes deformation in TE and signifies the deformation mode prevailing in the process. Nevertheless, it was shown with the aid of marker-insert experiments [20–22] that deformation in TE can remarkably deviate from the ideal deformation. In those marker-insert experiments, prior to processing, several metallic markers were inserted into the sample parallel to the extrusion axis. If deformation in TE followed the simple shear model (shearing–reverse shearing), the markers would preserve their arrangement in respect to each other and to the matrix after every TE pass. On the contrary, significant departure of the markers from their initial arrangement was found, which thereby signified deviations from the ideal deformation supposed by the simple shear model.

To account and predict the deviations from the ideal deformation in TE, Beygelzimer et al. [20] proposed a mathematical model that maps material points (or markers) from their initial configuration (with coordinates X and Y) into a deformed configuration (with coordinates x and y) within a cross section (Figure 2(a) and 2(b)). The model can be written in a general form as

$$\begin{aligned} x &= f(X, Y), \\ y &= g(X, Y). \end{aligned} \quad (1)$$

Mapping functions f and g can be in a simple polynomial form with fitting parameters definable from experimentally measured coordinates of the deformed markers. A more physically based approach, however, is to build the mapping functions with the use of kinematically admissible velocity fields as suggested by Beygelzimer

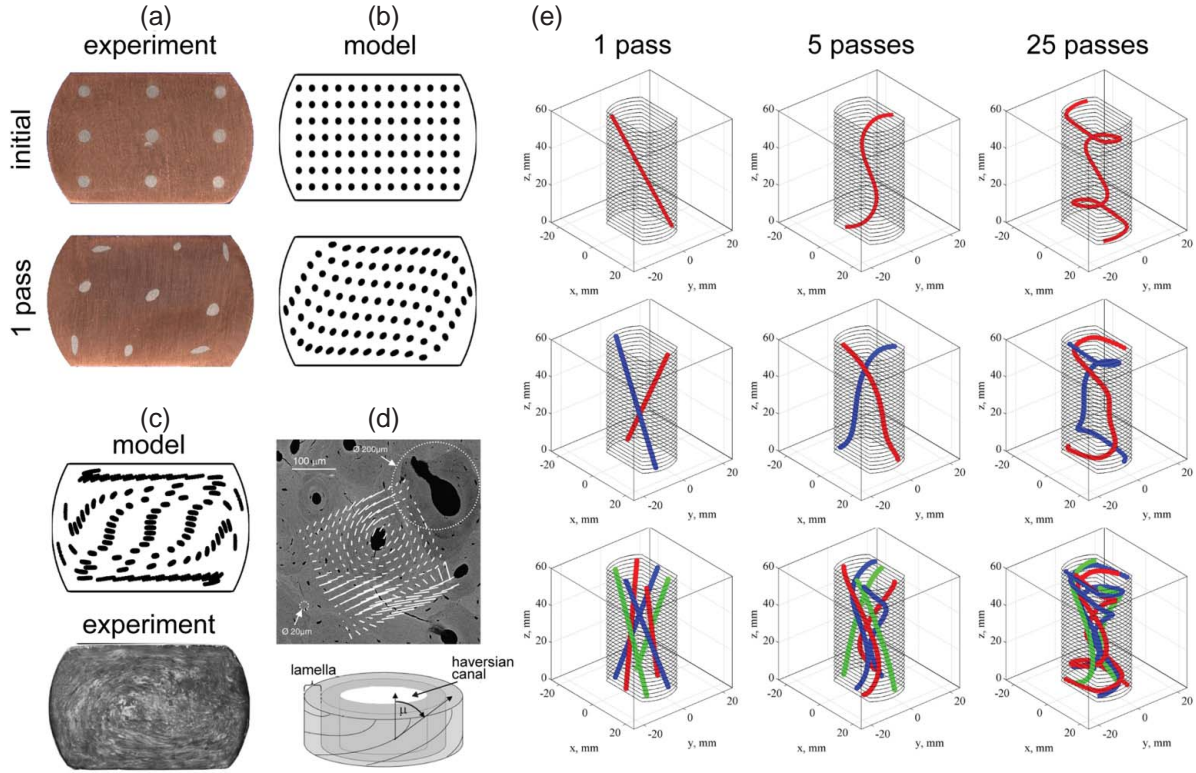


Figure 2. (a) Metallographic sections obtained in the marker-insert experiments [22]; (b) initial regular and deformed point sets obtained by mathematical mapping based on the experimental data [21]; (c) comparison between the microstructure of an Al sample after four passes [23] and a deformed point set after seven passes predicted by mathematical mapping [21]; (d) human compact bone with mineral particles around an osteon and a model of fibers of lamellae of an osteon [8]; and (e) initially straight fibers and prediction of their deformed configurations after 5 and 25 passes obtained in the present work by the mathematical model (Equation (2)).

et al.[20] In this approach, the coordinates of material points after deformation can be obtained through integration of a velocity field \vec{V} :

$$\begin{aligned} \frac{dx}{dt} &= V_x = \frac{\partial(\omega P)}{\partial y} - \frac{yV_0 \tan \beta}{R}, \\ \frac{dy}{dt} &= V_y = -\frac{\partial(\omega P)}{\partial x} + \frac{xV_0 \tan \beta}{R}, \\ \frac{dz}{dt} &= V_z = V_0. \end{aligned} \quad (2)$$

In Equation (2), twist-line slope, β , and the size of the channel cross section, R , define the geometry of the twist channel of the die; V_0 is the speed of the sample in the extrusion direction (ED), ω is a shape function of the twist channel ($\omega = 0$ on the surface of the channel, $\omega > 0$ within the channel, and $\omega < 0$ elsewhere), and P is a function to be minimized for fitting the theoretical predictions to the experimental data through a single adjustable parameter (see [20] for more details). The set of equations in Equation (2) is solved with $x(0) = X, y(0) = Y, z(0) = Z$ as the initial conditions. Equation (2) was obtained with an assumption of planar flow which supposes that sample cross sections normal to the ED remain planar during deformation. This

assumption is reflected in Equation (2) in the expression for the component of the velocity field along the ED, $V_z = V_0$.

The described model proved to be useful for understanding the complex material flow during TE and thus the morphology of microstructural features in the processed material (Figure 2(c)).[21]

Mathematical Modeling We shall now illustrate how the mathematical model described in Background section theoretically predicts the potential of TE for architecturing of composite materials. In Equation (1), the cross-sectional coordinates of the undeformed fibers, X and Y , were assumed to be independent of the position along the sample axis, Z . This assumption was used because, in the marker-insert experiments, the marker fibers were parallel to the sample axis prior to TE and, therefore, their initial coordinates were constant along the whole length of the sample. However, if the fibers are not parallel to the sample (and extrusion) axis prior to deformation, their cross-sectional coordinates in the undeformed configuration depend on the third coordinate, Z . In the case of fibers non-parallel to the extrusion

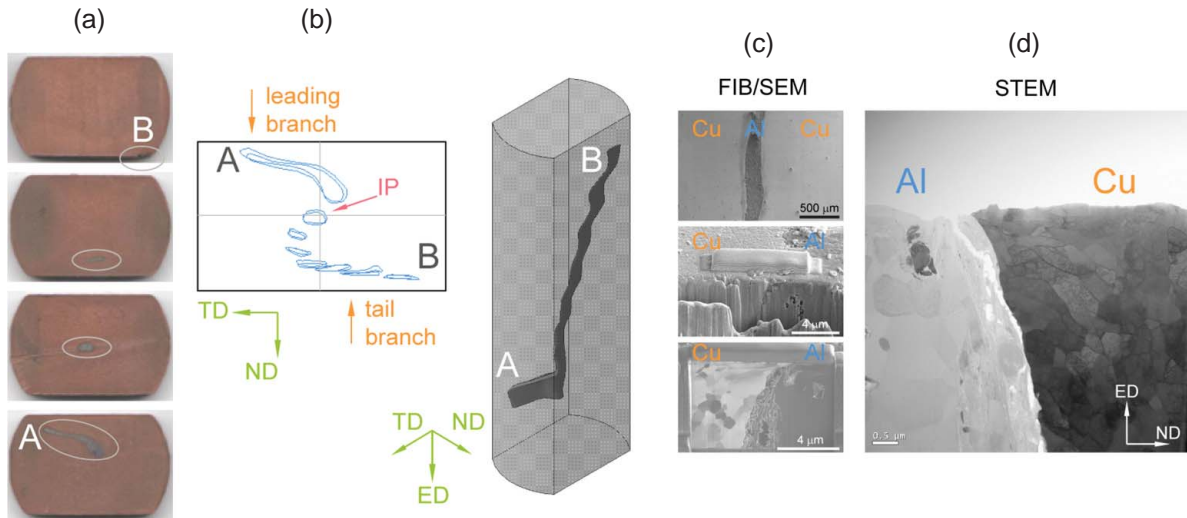


Figure 3. Experimental characterization of the composite after five TE passes: (a) photographs of metallographic sections of the composite; (b) contours of the Al fiber from scans of the metallographic sections (IP indicates the intersection point between fiber and composite axis); (c) approximate 3D reconstruction of the fiber shape; (d) FIB/SEM and TEM images of the contact between the Cu matrix and Al fiber in the corner region.

axis, Equation (1) becomes

$$\begin{aligned} x &= f(X(Z), Y(Z)), \\ y &= g(X(Z), Y(Z)). \end{aligned} \quad (3)$$

Mapping functions f and g can again be obtained from the kinematically admissible velocity fields (Equation (2)) fitted to experimental measurements of coordinates of the markers. Several examples of the use of the proposed mathematical model (Equation (3)) are illustrated in Figure 2(e). The simplest case is a single straight fiber diagonally inserted into the matrix. The model predicts that the initially straight but inclined fiber will assume a helical shape after five passes and a complex curled shape after 25 passes. In the same fashion, deformed configurations can be predicted for the case of multiple fibers inserted into the matrix. The results of mathematical modeling suggest that complex entangled reinforcements can be obtained in the composite in the case of two or more fibers inserted into the matrix for multi-pass TE (Figure 2(e)). Altogether, the predictions of the mathematical model, which was calibrated with the experimental data, clearly indicate that multi-pass processing by TE can be used for producing architected composites with helical or entangled reinforcements.

Experimental Realization For testing the theoretical predictions of architecturing by TE, multi-pass TE was performed on a composite consisting of a copper matrix and a single aluminum fiber. The preform composite was obtained by embedding the fiber into the matrix prior to TE at 45° (Figure 1(b)). The fiber was embedded by drilling a channel of a diameter of 1.5

mm in the matrix and filling the channel with an aluminum wire of nearly the same diameter. Both copper and aluminum were assembled into the composite in their as-received states and processed by TE without any prior heat treatment. Since the mathematical model predicted that five TE passes yield a sufficiently curved helicoidal shape of the fiber (Figure 2(e)), processing of the actual Al/Cu composite was also conducted up to five passes. Each TE pass was carried out at a temperature of $\sim 65^\circ\text{C}$ with a backward pressure of 230 MPa. The processed composite was sectioned into 3-mm sections for analyzing the deformed configuration of the fiber after multi-pass TE.

Figure 3(a–c) presents the results of the metallographic analysis of the deformed configuration of the fiber. The deformed configuration is significantly different from the initial straight shape and rather unexpected in the light of the theoretical predictions (Figure 2(e)). Observations of the deformed shape of the fiber can be summarized as follows. First, projection of the fiber cross sections from all metallographic slices on transverse direction–normal direction (TD–ND) plane (Figure 3(b)) shows that the fiber assumed a helicoidal shape along the ED. Second, the fiber intersects the axis of the composite and can be considered to consist of two branches that connect at the fiber–axis intersection. According to Figure 3(a–c), one branch located in the tail half of the composite (‘tail branch’, B) somewhat resembles the predicted helicoidal shape (Figure 2(e)). At the same time, the second half of the fiber (‘leading branch’, A) is very distinct from both the other half and the predicted shape. Indeed, instead of a helicoidal shape, the end part of the fiber became almost parallel to the TD–ND plane (normal to the extrusion axis).

This fact is especially clear in a photograph of the corresponding section of the composite (Figure 3(a)). In other words, the deformed fiber had a helicoidal shape in the tail region of the composite, whereas toward the leading end of the composite, the fiber collapsed into a plane normal to the ED. To understand such an unexpected behavior of the fiber during multi-pass TE, FE simulations were performed and described in the next section.

On the experimental side, the contact region between the matrix and the fiber was also analyzed because the contact condition can have a considerable impact on the overall properties of composite materials. For examination of the contact region, one of the sections of the composite in which the fiber was located in a corner of the matrix was analyzed in a transmission electron microscope (TEM) and a scanning electron microscope (SEM) equipped with focused ion beam (FIB). Figure 3(d) presents FIB/SEM images and a scanning TEM bright-field image of the contact area taken in the corner area of the composite. It is seen that the copper matrix underwent significant grain refinement during the TE process, whereas somewhat larger grains are seen in the aluminum fiber. The images also reveal that processing with the present conditions did not result in mixing between the metals as could be expected from a previous work reporting mixing between the matrix and second-phase particles.[19]

FE Modeling The FE method has proved to be a powerful tool for analyzing various aspects of SPD processing [24,25] and therefore was employed in the current work for understanding of the material flow during multi-pass TE and for identifying factors responsible for the unexpected shape of the fiber observed experimentally. Three-dimensional FE simulations in the present study were performed with DEFORM 3D software, which offers powerful means for remeshing that was necessary in the present case of multi-pass TE involving large strains and distortions of elements.

The FE model contained a deformable sample and three rigid parts: a TE die, a punch for forward pressure, and a punch for backward pressure. In order to model the extrusion process, a constant velocity of 3 mm/s was prescribed to the forward punch in the ED, a constant force of 50 kN was applied to the backward punch in the counter-ED, and the TE die was fixed in space. Frictional interactions were defined between the tools and the sample with various friction factors: $k = 0.0$ between the punches and the sample and either $k = 0.0$ or $k = 0.08$ between the TE die and the sample. Multiple passes were simulated continuously without unloading stages. Given the low extrusion rate (3 mm/s) and relatively low temperature (65°C), at which actual processing was conducted, heat effects were not considered in the FE model.

The sample was assumed to contain only the matrix material, that is, the fiber was excluded from the current FE analysis for simplifying the computationally demanding problem. The assumption of negligible effects of the fiber on the overall deformation of the composite during TE was considered reasonable in the light of the small volume fraction and the soft material of the fiber (aluminum). Indeed, elastic and plastic strains in a composite containing soft particles and a harder matrix are almost as homogeneous as in the single-phase material.[26] With neglecting the fiber, the whole sample was assigned the following properties of the copper matrix: a Young modulus of 110 GPa, Poisson ratio of 0.34, and yield stress of 100 MPa. The material was considered to be isotropic and perfectly plastic with the von Mises yield criterion. The shape of the ‘fiber’ predicted by FE simulations was analyzed by tracing material points of the matrix that corresponded to the location of the fiber in the actual composite.

The results of the FE modeling of continuous multi-pass TE shed some light on the experimentally observed shape of the fiber (Figure 4(a)). The FE simulations show how the fiber deviates from its initial straight configuration and how the deviations accumulate with every consequent pass. From the second pass, the behavior of the two halves of the fiber starts to differ. While the tail branch of the fiber develops into the expected helicoidal shape, the leading branch of the fiber tends to curve in counter-ED. After the third pass, the leading branch lies in the TD–ND plane, which is very similar to the experimental observations (Figure 4(a)). After the fourth pass, the leading end of the fiber is further curved toward the tail, which makes the curvature of this part of the fiber very different from the result of the mathematical modeling (Figure 2(e)).

From these FE predictions, it is clear that the spiral shape of the fiber is distorted by shifts of some parts of the fiber in the counter-ED. These shifts might be associated with out-of-plane distortions of the cross sections normal to the ED, which were found in a previous FE study of TE.[18] Particularly, it was found that periphery regions of the sample cross sections lag behind the central regions during extrusion. Such out-of-plane distortions account for the deviations of the fiber configuration from the theoretical predictions. Indeed, it is seen from the FE results that both ends of the fiber are shifted in counter-ED (Figure 4(a)). Since the tail branch of the fiber is directed in the same counter-ED as the out-of-plane distortions, the effect of the shifts is less noticeable. At the same time, the leading branch of the fiber is directed in the ED so that the out-of-plane distortions reverse the curvature of the fiber to the opposite (Figure 4(a)).

Now that it is clear why the deformed configuration of the fiber is different from the theoretical prediction, the next objective for FE simulations was to optimize

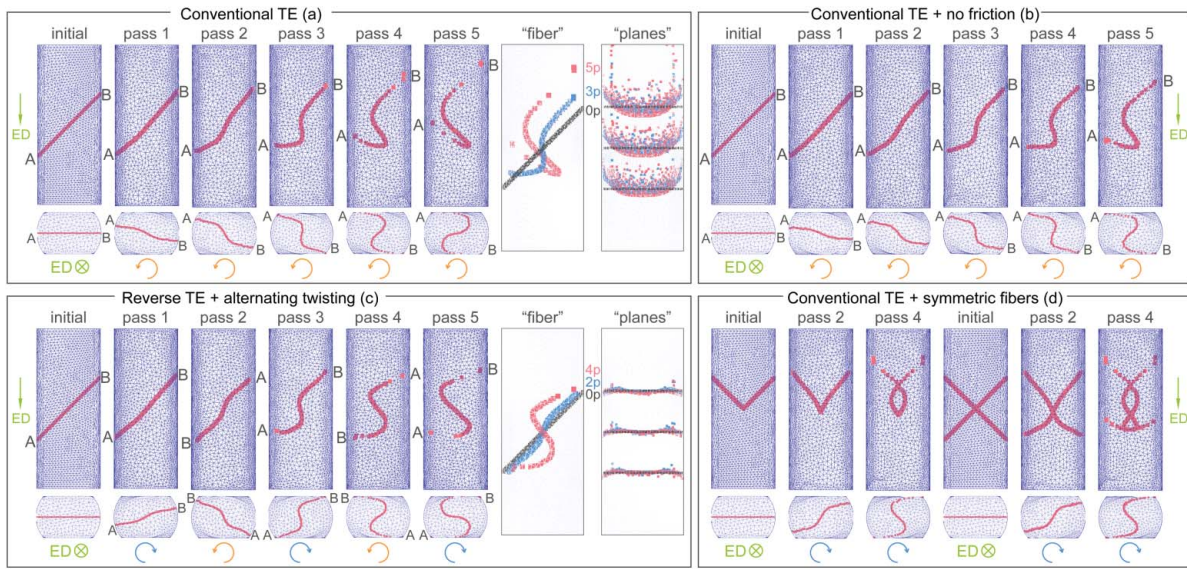


Figure 4. FE analysis of the evolution of the fiber shape during multi-pass TE by point tracing under different processing conditions: (a) conventional TE with the constant ED and friction factor $k = 0.08$; (b) the same with frictionless contact ($k = 0.00$); (c) reverse TE with alternating ED and the sense of twisting; (d) conventional TE for V-shaped and X-shaped fibers. In (a) and (c) cases, points corresponding to fibers and sample cross sections after various numbers of passes are superimposed.

the processing regime and the initial shape of the fiber for improved reinforcements in composites produced by multi-pass TE. The following ideas were tested.

- (1) Frictionless processing (Figure 4(b)). Friction was expected to intensify the deviations of the fiber shape from the theoretical shape and thus reducing friction was thought to lead to improved reinforcements. This expectation followed from the results of the previous study,[18] which showed that out-of-plane distortions depend on the friction condition between the sample and the die: distortions are more severe with higher values of the friction factor. The FE simulations performed in the current study reveal that reducing friction indeed leads to smaller shifts in the counter-ED; however, the final shape of the fiber is still different from the targeted well-shaped helix.
- (2) Reverse TE (not shown). It is clear that the fiber shape deviates from the theoretical one because of the out-of-plane distortions that accumulate during multi-pass extrusion in the same direction. Therefore, reversing the ED after each pass may balance the out-of-plane distortions. The FE simulations of the reverse TE suggest, however, that not only distortions are balanced, but also the fiber restores its original configuration after each even (second, fourth) pass of TE. In other words, such processing results in a nearly straight shape of the fiber, similar to the initial configuration.

- (3) Reverse TE with alternating sense of twisting (Figure 4(c)). From the described FE analysis, it appears that both the ED and the sense of twisting should be changed to the opposite after every TE pass (Figure 1(c)). Such processing is expected to prevent significant out-of-plane distortions in a single direction and, at the same time, to form a desired helicoidal reinforcement. The FE simulations of reverse TE with alternating sense of twisting reveal that, indeed, a well-shaped helicoidal fiber can be obtained after such a TE process. The improved fiber shape follows from balanced out-of-plane distortions after each even pass as a result of reversing the ED (Figure 4(c)).
- (4) Initially symmetric fibers (Figure 4(d)). The composite processed in the current experiments arrived at a highly asymmetrical configuration because of the initially asymmetrical shape of the fiber in respect to the extrusion axis. It follows that a more beneficial reinforcement can be obtained if the fiber initially has a twofold symmetry in respect to the extrusion axis. V- and X-shaped fibers are examples of such fibers with the twofold symmetry, for which the FE simulations predict interesting reinforcements after conventional multi-pass TE.

Discussion and Outlook The modeling and experiments presented in the previous sections demonstrate that multi-pass TE has a potential for architecturing of helicoidal fiber composites. Indeed, the mathematical

model (calibrated by experimental data) predicted that straight fibers non-parallel to the extrusion axis will assume helical or entangled shapes after multiple TE passes (Figure 2(e)). At the same time, the pilot experiments with a copper matrix and a single aluminum fiber revealed an unexpected configuration of the fiber (Figure 3). The FE simulations, which captured the experimental observations much better (Figure 4), suggested that out-of-plane distortions of the sample cross sections are responsible for the significant difference between the experimental results and the theoretical predictions in multi-pass TE. Indeed, the mathematical model used for the shape transformation of the fiber was developed with the assumption of no out-of-plane distortions (Background section). Finally, based on the FE analysis, the following measures were proposed to improve reinforcements in twist-extruded composites: (i) reverse TE with alternating sense of twisting and (ii) fibers with twofold symmetry in respect to the extrusion axis.

With the optimized processing regimes, TE promises to achieve helicoidal reinforcements in metal–matrix composites. Such composites are beneficial for several reasons. First, composites reinforced by helical fibers can enjoy additional strain hardening provided by geometry alone.[6] Such geometry-induced strain hardening allows postponing plastic instabilities (e.g. necking) in the material during deformation. Furthermore, the fact that the helicoidal design of structures is advantageous is reflected in it being widespread in biomaterials built by different species.[8] Examples of helicoidal structures include molecules such as DNA and collagen [9]; helicoidal design of fiber composites is found in wood, human bone osteon (Figure 2(d)),[8] equine hoof, and sea sponge.[9] The helicoidal character of fiber arrangement in wood cells or bone osteon makes these biostructures extensible and compressible along the axis, like springs, and helps protection of inner canals for blood or water and nutrient transport.[8]

The present work also demonstrates that architecturing of composites in TE can be accompanied by considerable grain refinement (Figure 3(d)) as well as microstructural gradients in both matrix and fibers. Altogether it makes multi-pass TE a uniquely appropriate SPD route for realization of the concept of simultaneous architecturing and nanostructuring in bulk metallic materials. In the current experiments, the architected composite consisted of a copper matrix and a single aluminum fiber, which were used for the purpose of merely testing the idea of architecturing by TE. Future work aimed at producing architected materials with superior properties should engage more advantageous pairs of materials, for example, stiff fiber material and ductile matrix material. Furthermore, it can be recommended to increase the volume fraction of the fibers for a more pronounced reinforcement effect. An increase in

the volume fraction can be gained through enlargement of the fibers or through an increase in their number. Insertion of powders instead of bulk fibers into the channels of the matrix can also be considered, especially in the cases of initially complex channels (e.g. V and X shapes, Figure 4(d)).

Finally, the interface between the fiber and the composite also deserves attention. A previous report [19] suggested that deformation during TE may facilitate mutual mixing of dissimilar materials and strong bonding, which however was not observed in the current experiments (Figure 3(d)). The lack of mixing and bonding in the obtained composite may have resulted from aluminum oxides on the surface of the fiber. Therefore, in order to improve bonding between the matrix and fibers in extruded materials, special surface preparation or heat treatment procedures can be considered to complement mechanical processing by multi-pass TE.

In conclusion, the concept of architecturing of composites by multi-pass TE is introduced. The results of the present work demonstrate the promise of the proposed method for manufacturing metal–matrix composites with various non-trivial reinforcements. Based on the FE analysis, reverse TE with alternating sense of twisting is recommended for obtaining well-shaped helicoidal reinforcements. Fibers with twofold symmetries in respect to the extrusion axis were also found to yield interesting results. The present work is anticipated to invite further research dedicated to development of the proposed technology for producing architected composites with superior properties.

Acknowledgements The authors wish to thank Y. Gusar, D. Prilepo, A. Gumennyi, and P. Gumennyi for their help in processing by TE. This work was supported by the National Research Foundation of Korea (NRF) grant funded by the Korea government (MSIP) (No. 2014R1A2A1A10051322).

Disclosure Statement No potential conflict of interest was reported by the authors.

ORCID

Marat I. Latypov  <http://orcid.org/0000-0003-4416-0877>

Hyoungh Seop Kim  <http://orcid.org/0000-0002-3155-583X>

References

- [1] Bouaziz O, Bréchet Y, Embury JD. Heterogeneous and architected materials: a possible strategy for design of structural materials. *Adv Eng Mater.* 2008;10:24–36.
- [2] Brechet Y, Embury JD. Architected materials: expanding materials space. *Scr Mater.* 2013;68:1–3.
- [3] Wu X, Jiang P, Chen L, Yuan F, Zhu YT. Extraordinary strain hardening by gradient structure. *Proc Natl Acad Sci.* 2014;111:7197–7201.
- [4] Wang HT, Tao NR, Lu K. Architected surface layer with a gradient nanotwinned structure in a Fe–Mn austenitic steel. *Scr Mater.* 2013;68:22–27.

- [5] Wei Y, Li Y, Zhu L, Liu Y, Lei X, Wang G, Wu Y, Mi Z, Liu J, Wang H, Gao H. Evading the strength-ductility trade-off dilemma in steel through gradient hierarchical nanotwins. *Nat Commun.* 2014;5. Article ID 3580.
- [6] Bouaziz O. Geometrically induced strain hardening. *Scr Mater.* 2013;68:28–30.
- [7] Dyskin A, Estrin Y, Pasternak E, Khor HC, Kanel-Belov AJ. Fracture resistant structures based on topological interlocking with non-planar contacts. *Adv Eng Mater.* 2003;5:116–119.
- [8] Fratzl P, Weinkamer R. Nature's hierarchical materials. *Prog Mater Sci.* 2007;52:1263–1334.
- [9] Meyers MA, Chen P-Y, Lin AY-M, Seki Y. Biological materials: structure and mechanical properties. *Prog Mater Sci.* 2008;53:1–206.
- [10] Dunlop JWC, Fratzl P. Multilevel architectures in natural materials. *Scr Mater.* 2013;68:8–12.
- [11] Fleck NA, Deshpande VS, Ashby MF. Micro-architected materials: past, present and future. *Proc R Soc A.* 2010;466:2495–2516.
- [12] Ashby M. Designing architected materials. *Scr Mater.* 2013;68:4–7.
- [13] Bouaziz O, Kim HS, Estrin Y. Architecturing of metal-based composites with concurrent nanostructuring: a new paradigm of materials design. *Adv Eng Mater.* 2013;15:336–340.
- [14] Kimura Y, Inoue T, Yin F, Tsuzaki K. Inverse temperature dependence of toughness in an ultrafine grain-structure steel. *Science.* 2008;320:1057–1060.
- [15] Valiev RZ, Alexandrov IV, Zhu YT, Lowe TC. Paradox of strength and ductility in metals processed by severe plastic deformation. *J Mater Res.* 2002;17:5–8.
- [16] Liddicoat PV, Liao X-Z, Zhao Y, Zhu Y, Murashkin MY, Lavernia EJ, Valiev RZ, Ringer SP. Nanostructural hierarchy increases the strength of aluminium alloys. *Nat Commun.* 2010;1:63.
- [17] Beygelzimer Y, Orlov D, Varyukhin V. A new severe plastic deformation method: twist extrusion. In: Zhu YT, Langdon TG, Mishra RS, Semiatin SL, Saran MJ, Lowe TC, editors. *Ultrafine grained materials II. Proceedings*; 2002 Feb 17–21; Warrendale (PA): The Minerals, Metals & Materials Society; 2002.
- [18] Latypov MI, Lee M-G, Beygelzimer Y, Kulagin R, Kim HS. On the simple shear model of twist extrusion and its deviations. *Met Mater Int.* 2015;21:569–579.
- [19] Beygelzimer Y, Varyukhin V, Synkov S, Orlov D. Useful properties of twist extrusion. *Mater Sci Eng A.* 2009;503:14–17.
- [20] Beygelzimer Y, Reshetov A, Synkov S, Prokof'eva O, Kulagin R. Kinematics of metal flow during twist extrusion investigated with a new experimental method. *J Mater Process Technol.* 2009;209:3650–3656.
- [21] Kulagin R, Latypov MI, Kim HS, Varyukhin V, Beygelzimer Y. Cross flow during twist extrusion: theory, experiment, and application. *Metall Mater Trans A.* 2013;44:3211–3220.
- [22] Kulagin R. Improving the technology and equipment for the twist extrusion process based on the analysis of the billet deformed state [dissertation]. Donetsk, Ukraine: Donetsk Institute for Physics and Engineering; 2014.
- [23] Orlov D, Todaka Y, Umemoto M, Beygelzimer Y, Tsuji N. Comparative analysis of plastic flow and grain refinement in pure aluminium subjected to simple shear-based severe plastic deformation processing. *Mater Trans.* 2012;53:17–25.
- [24] Kim HS, Joo S-H, Jeong HJ. Plastic deformation and computer simulations of equal channel angular pressing. *Kor J Met Mater.* 2014;52:87–99.
- [25] Yoon SC, Horita Z, Kim HS. Finite element analysis of plastic deformation behavior during high pressure torsion processing. *J Mater Process Technol.* 2008;201:32–36.
- [26] Kim HS, Hong SI, Kim SJ. On the rule of mixtures for predicting the mechanical properties of composites with homogeneously distributed soft and hard particles. *J Mater Process Technol.* 2001;112:109–113.